iJRASET
International Journal For Research in Applied Science and Engineering Technology



INTERNATIONAL JOURNAL FOR RESEARCH

IN APPLIED SCIENCE & ENGINEERING TECHNOLOGY

Volume: 11 **Issue:** VI **Month of publication:** June 2023

DOI: https://doi.org/10.22214/ijraset.2023.54229

www.ijraset.com

Call: 08813907089 | E-mail ID: ijraset@gmail.com

International Journal for Research in Applied Science & Engineering Technology (IJRASET)
ISSN: 2321-9653; IC Value: 45.98; SJ Impact Factor: 7.538
Volume 11 Issue VI Jun 2023- Available at www.ijraset.com

Effect of Temperature Variation on Rigid Pavement by using Sensor

Mr. Aditya Nanaware[1], Prof. Rajshekhar Rathod[2], Prof. Achyut Deshmukh[3]
[1]M. Tech Student, [2]Head of Department, [3]Asst. Professor, Civil Engineering Department, MIT ADT University, Pune, Maharashtra India

Abstract: ***Variations in temperature have an impact on both stiff and flexible pavements. Although the main component of pavements is crushed stone aggregate, which is not temperature-sensitive, the binder that holds the aggregates together is more temperature-sensitive. Pavements made of Portland cement concrete (PCC) that are cast in the field experience volume fluctuations as a result of changes in temperature and moisture. Utilize sensors to examine the impact of temperature and moisture change on stiff pavement. Analyze the technical and physical characteristics of sensors. locating sensors in solid pavement in order to get accurate data. This research aims to analyze temperature differences for stiff pavement (mainly for the PQC layer). Table 1 in IRC:58-2015 lists the temperature differences for several Indian areas. In order to design pavement slabs of varied thicknesses, it offers temperature differential values. However, the table's footer also states that the data was collected in 1974 by the Government Road Experiment Station in New Delhi. This analysis is done to compare the temperature difference between that table, which is over 50 years old, and the present temperature. It has been noted that temperature measurements obtained from a temperature sensor closely match the information provided by the metrological department. (Data on temperatures from July to November) Data from the prior 10 years are collected for further examination when data from the IMD is confirmed to be the same (2012 to 2021). The temperature disparity over the next 10 years is forecasted using those data (2022 to 2031). When compared to IRC, data have revealed a rise in the minimum and maximum temperature disparity.***
Keywords: Temperature Sensor, concrete, temperature stress, temperature gradient, thermocouples and Digital thermometer.

I. INTRODUCTION

Temperature variations affect both rigid and flexible pavements. Though pavements primarily consist of crushed stone aggregates, which are not reactive to temperature, the binder used to bind the aggregates is more dependent on temperature. When Portland cement concrete (PCC) pavements are cast in the field, they undergo volume changes because of temperature and moisture variations. The restrained volume changes cause stress developments in a pavement system, and random cracking occurs if the developed tensile stress surpasses the tensile strength of concrete. Temperature and moisture have impact on concrete slab to monitor these parameters structural health monitoring (SHM) processes have been designed. Which determines the status of structures to increase their service life and safety level? Hence, SHM is a very effective tool to increase the confidence level of the condition of structures. During the past few decades, development in the transportation industry compelled the world to focus on monitoring road pavement and providing a sustainable transportation network. The increase in information and sensing technology led the world to invent advanced monitoring systems for road pavement. Besides, pavement monitoring is the first step in the pavement treatment process; it has an effective side of maintenance and has a significant role in the development of transportation systems. Pavement monitoring focusses mainly on surface distresses, texture, patching, friction, surface thickness and vehicle volume. sensors were installed to collect structural information and after the stress analysis the collected information was used for identification of critical locations presented an OSP of TYTON joints of water pipeline subjected to near and far field earthquakes. In this study OSP was considered in TYTON joints to detect seismic damage. They evaluated a new method for OSP based on nonlinear time-history analysis results as an accurate seismic response.

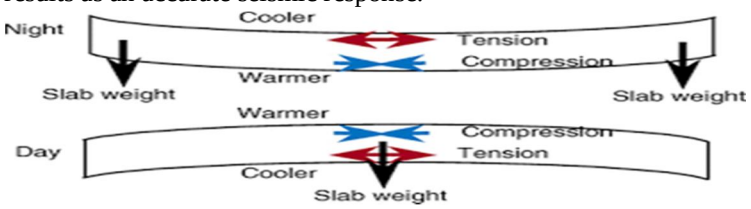


Figure No.1 Temperature stress

©IJRASET: All Rights are Reserved

ISSN: 2321-9653; IC Value: 45.98; SJ Impact Factor: 7.538
Volume 11 Issue VI Jun 2023- Available at www.ijraset.com

A. Rigid Pavement

Rigid pavements have sufficient flexural strength to transmit the wheel load stresses to a wider area below. The design is based on flexural strength and deformation in the sub grade is not transferred to subsequent layers. Thermal stresses are more susceptive to be induced as the ability to contract and expand is very less in concrete. Force of friction is high.

Rigid pavements are constructed of Portland cement concrete slabs resting on a prepared subbase of granular material or directly on a granular subgrade. Load is transmitted through the slabs to the underlying subgrade by flexure of the slabs. Flexible pavements are constructed of several thicknesses…

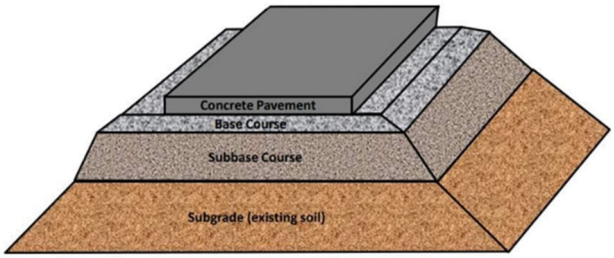


Figure No.2 Rigid Pavement

B. In-pavement Surface Temperature and Condition Sensor

Passive Road Surface Sensor provides actionable information about the roadway to road weather professionals. The sensor is installed in the roadway and measures the surface temperature and the surface condition as dry, wet, ice watch and chemically wet. The sensor is well suited for roadways, ice-prone bridges, and elevated roadways, entryways, parking garage ramps and loading docks.



Figure No.3 In-Pavement Surface Temperature and Condition Sensor

The road surface sensor connects to signal conditioning modules for connection to HSE's line of data loggers. The signal conditioning modules are DIN rail mountable and can be provided in a mountable enclosure as an option. The surface sensor measuring elements are molded in a resilient epoxy compound with thermal properties that closely match the roadway surface. It works on thermally passive principles; no artificial heating or cooling is used that may alter the measured environment. The maintenance-free design features corrosive-resistant electrodes to derive the presence of moisture on the roadway surface.

C. Temperature and moisture sensors

Company "Interpribor" produced temperature and moisture sensors on the order of Kazakhstan Highway Research Institute. Each sensor, produced in the form of metal capsule, contains element for measurement of temperature based on the effect of thermal resistance and element for measurement of moisture through diamagnetic permeability. Such design concept allows performing the measurement of temperature and moisture simultaneously in points of pavement and subgrade.

©IJRASET: All Rights are Reserved

ISSN: 2321-9653; IC Value: 45.98; SJ Impact Factor: 7.538
Volume 11 Issue VI Jun 2023- Available at www.ijraset.com



Figure No. 4 Technical systems for temperature and moisture measurement's a– one set of temperature and moisture sensors; b – surface measurement part.

Temperature elements of sensors were calibrated by the producer, and moisture elements were calibrated in the laboratory of KazdorNII. Calibration of sensors was performed with the use of soils, selected from the location of their installation. Installation of sensors into pavement and subgrade layers of the highway was performed by the specialists of KazdorNII. Measurement ends of the sensors were put on the surface of the highway and collected in measurement chamber of land system of the set. The set had 11 temperature and moisture sensors, 3 of which were installed into the pavement layers and 8 of them were installed into the subgrade of the highway. The depths for their installation were equal to 2, 12, 23, 35, 70, 105, 140, 175, 210, 245 and 280 cm.

II. LITERATURE REVIEW

Karthikeyan Loganathan et.al the surface temperature of pavements is a critical attribute during pavement design. Surface temperature must be measured at locations of interest based on time-consuming field tests. The key idea of this study is to develop a temperature profile model to predict the surface temperature of flexible and rigid pavements based on weather parameters. Determination of surface temperature with traditional techniques and sensors are replaced by a newly developed method. The method includes the development of a regression model to predict the average annual surface temperature based on weather parameters such as ambient air temperature, relative humidity, wind speed, and precipitation. Detailed information about temperature and other parameters are extracted from the Federal Highway Administration's (FHWA) Long Term Pavement Performance (LTPP) online database. The study was conducted on 61 pavement sections in the state of Alabama for a 10-year period. Audrius Vaitkus et.al Environmental conditions (temperature, moisture and the intensity of the sun) influence variation in asphalt pavement strength during the year. Lithuania is situated in a zone by average warm summers and average cold winters, and the most important climatic factor is the variation of the air temperature. This study presents the influence of temperature (of asphalt concrete (AC) and subgrade layers) and moisture content (of subgrade layers) to the pavement bearing capacity. The experimental research was obtained in five pavement sections of the experimental road. This experimental road was constructed in 2007 in Lithuania and is operated for more than 12 years. This paper presents a statistical analysis between the bearing capacity and the thickness of the asphalt concrete layers, the temperature and moisture content of different pavement layers, among sections, loaded and unloaded lanes (right and left wheel paths and tracks). Liping Liu et.al Temperature is one of the most important factors affecting functional as well as structural performance of asphalt pavements with thick asphalt layer (>30 cm). For a successful pavement design, it is vital to accurately predict the pavement temperatures at various depths. However, most previous researches focused on the temperature predictions for conventional asphalt pavements, of which the asphalt thickness is less than 30 cm. This suggests their proposed models are applicable in top layers, but may not be so effective for temperature predictions at deeper depths. As a result, the primary objective of this research was to develop a statistical model to predict temperatures at deep depths. Three test sites were selected, and they were instrumented with a number of sensors and a data logger to record the pavement temperature hourly. Also, all test sections can provide meteorological monitoring to collect hourly air temperatures and hourly total solar radiation.

Prakash Somani et.al Due to an increase in the population, the need for good and efficient transportation becomes essential to provide better facilities to the people. Nowadays, concrete pavements are more adopted in highway construction.

©IJRASET: All Rights are Reserved

ISSN: 2321-9653; IC Value: 45.98; SJ Impact Factor: 7.538
Volume 11 Issue VI Jun 2023- Available at www.ijraset.com

The concrete pavement is more efficient because of its higher strength, durability, and reliability, but concrete pavements are largely affected due to temperature stresses. This study investigates the potential use of phase changing material (PCM) for the reduction of temperature stresses in concrete pavements. To inspect compressive strength and temperature differential of concrete mixes at different substitution levels of PCM. An indoor heat simulator with temperature sensors was used to measure the temperature differential of concrete mixes. The temperature differential is a major factor for generating curling in concrete pavement. Results recommend that increment in PCM content reduces the temperature stresses in concrete pavement. Sumit Gupta et.al and to use electrical resistance tomography (ERT) for characterizing spatially distributed damage during accelerated pavement testing. This self-sensing concrete not only retains the expected mechanical properties of typical airport pavements, but it can also sense deformation and strain. First, sensing properties were encoded in concrete pavements by modifying the cement-aggregate interface with multi-walled carbon nanotube (MWCNT) thin films. MWCNT thin films were spray-coated onto dried fine and coarse aggregates, and the film-coated aggregates were directly used for concrete casting. Second, an ERT algorithm was implemented for spatial conductivity mapping of self-sensing concrete pavements. Extensive laboratory tests were conducted on different sized specimens for characterizing their spatial damage detection performance. Last, a full-scale concrete airport pavement slab was cast with self-sensing concrete patches at locations where damage was expected. A heavy vehicle simulator was employed for accelerated pavement testing to induce cracks, while ERT measurements were collected at periodic intervals during testing.

III. METHODOLOGY

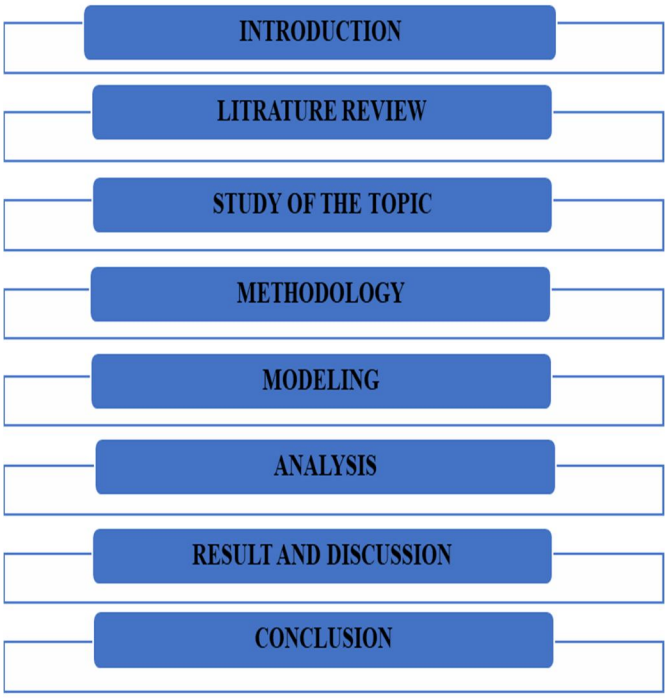


Figure No.5 Methodology Flowchart

A. Data Collection

In order to analyze the performance on continuous data collection, six samples were made and four digital temperature sensors installed on each of test samples and temperature measured over a 5 months' period (July 2022 – November2022). The samples were constructed in open environment to study the temperature variations. The samples' data was collected eight times a day along with meteorological information from a nearby station (air temperature, rain, wind, etc.). All registered measurements were combined into a database for further analysis of temperature diffusivity on pavement.

Depicts the behavior of daily average temperature for each probe over a year. It is clearly illustrated that the average temperature evolves as expected for each sensor, reaching the minimum and maximum values around November and August, respectively. Moreover, despite being only 2 m apart from each other, a slight difference can be appreciated among temperature evolution in each Sample. This is explained by the different pavement materials.

©IJRASET: All Rights are Reserved | SJ Impact Factor 7.538 | ISRA Journal Impact Factor 7.894 |

IV. RESULT AND DISCUSSION

A. Ansys Model

1) Thermal Stress Analysis from Year (2012 To 2021)Geometry

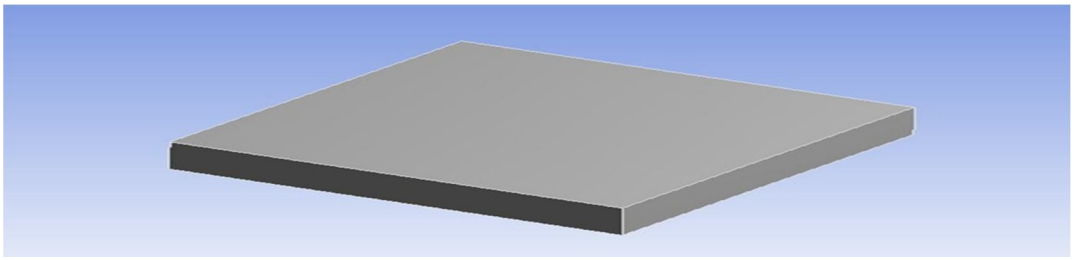


Figure.6 Geometry

2) Meshing

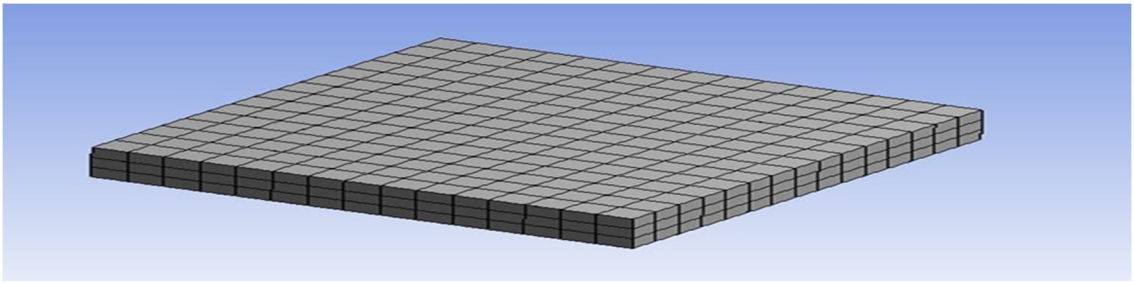


Figure.7 Meshing

Meshing, known as mesh generation, is the process of generating a two-dimensional and three- dimensional grid; it is dividing complex geometries into elements that can be used to discretizea domain. In meshing the model is divided in 3712 number of nodes and 675 numbers of elements.

B. Boundary Condition

1) Transient Thermal Temperature

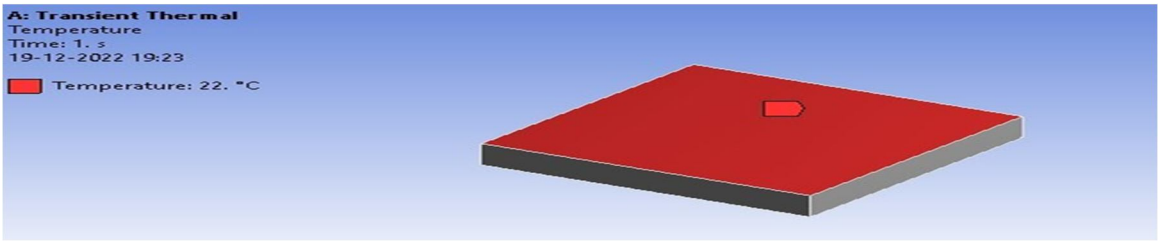


Figure.8 Transient Thermal Temperature

In steady-state heat transfer, the temperature is constant throughout time. In transient heat transfer, the temperature changes with time. Temperature applied in boundary condition is 22^0C.

2) Standard Earth Gravity

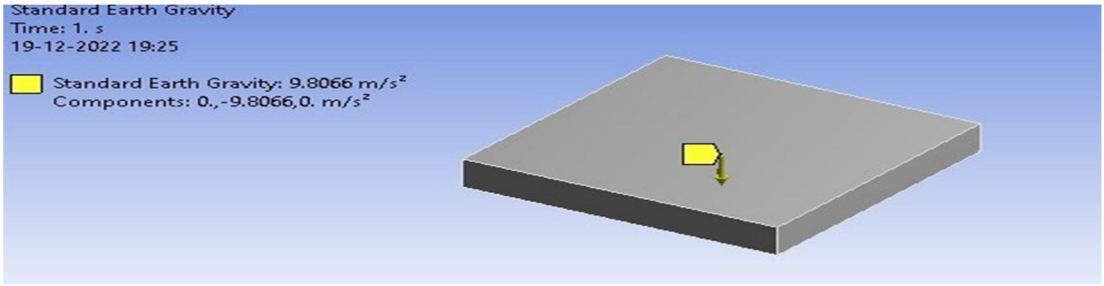


Figure.9 Standard Earth Gravity

The nominal value of standard gravity is, by definition, 9.80665 m/s2 (32.1740 ft/s2). Fixed support

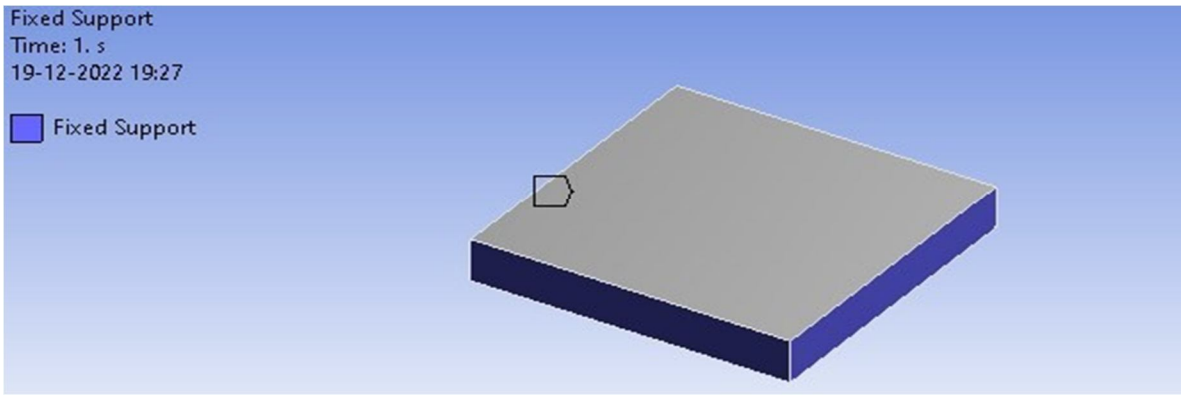


Figure.10 Fixed Support.

A fixed support is the most rigid type of support or connection. It constrains the member in alltranslations and rotations (i.e., it cannot move or rotate in any direction). The easiest exampleof a fixed support would be a pole or column in concrete. Fixed Support Means X, Y and Z are all set to 0. If have a plane of symmetry, that sets the displacement normal to that plane to 0. In this model fixed support applied at the side surfaces.

3) Thermal Condition

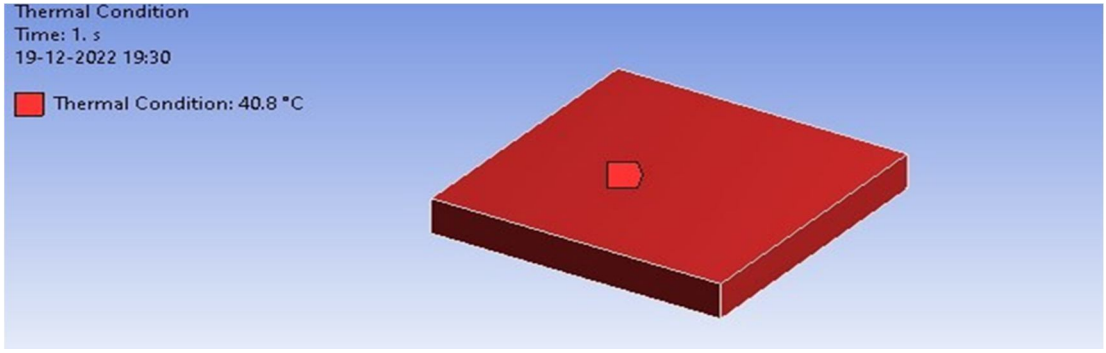


Figure.11 Thermal Condition

Ansys thermal analysis solutions help engineers solve the most complex thermal challenges topredict how their designs will perform with temperature changes. Account for temperature fluctuations. Prevent overheating issues. Improve product reliability across environments. In this model thermal condition applied is 40.8^{0}C.

C. Analytical Results For M40

1) Total deformation

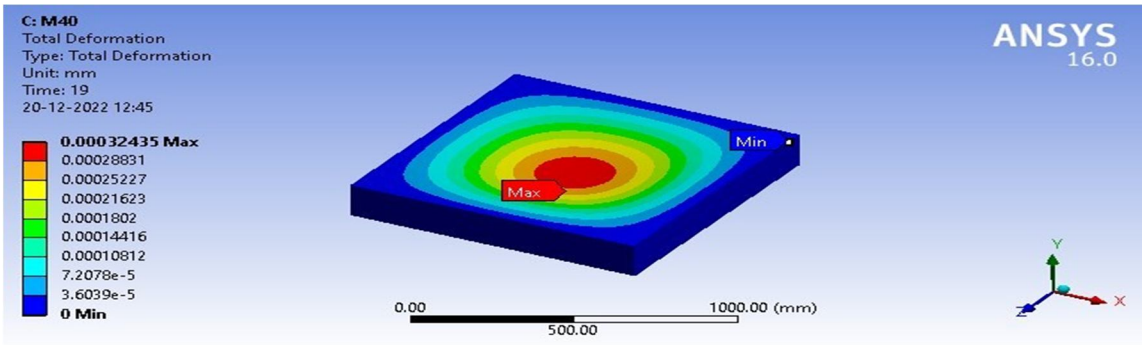


Figure.12 Total Deformation

The inclusion of total deflection means that ANSYS accounts for changes in stiffness due to changes in the shape of the parts you are simulating. The maximum deformation is 3.24 x 10^{-4}mm and minimum deformation is 3.60 x 10^{-5}mm.

2) Equivalent Stress

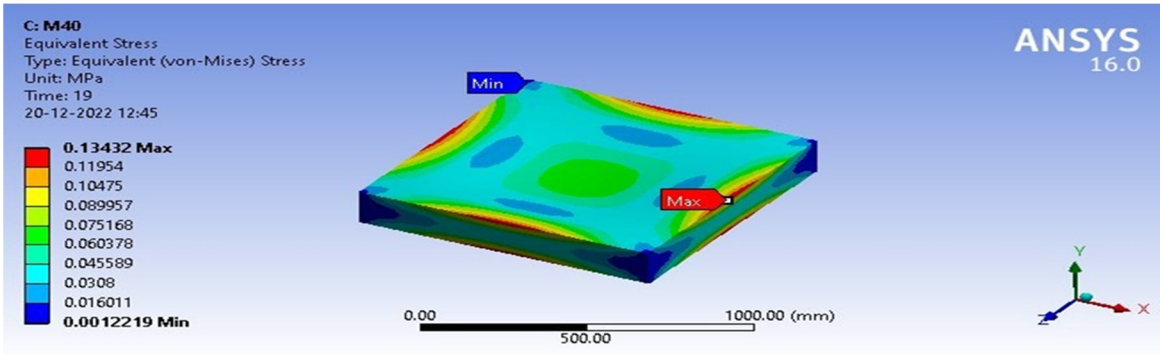


Figure.13 Equivalent Stress

Equivalent stress is widely used to represent a material's status for ductile material. Engineers use this simple scalar value to determine if the material has yield or failed. The maximum Equivalent Stress is 1.34 Mpa and minimum Equivalent Stress is 0.001219 Mpa.

3) Normal Stress

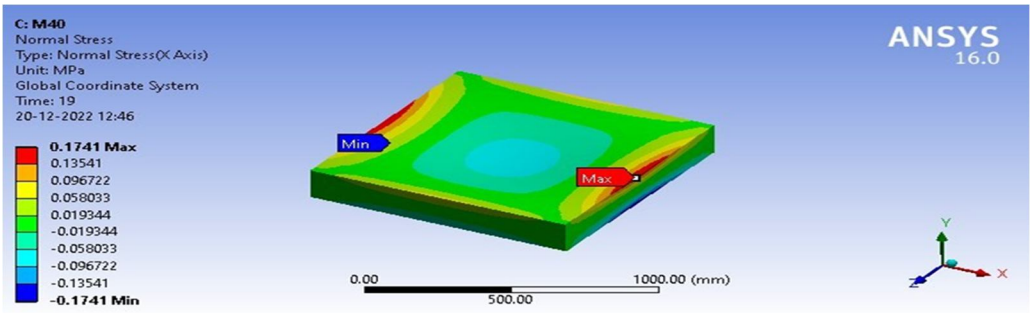


Figure.14 Normal Stress

Normal Stress might be useful is when you request stress on a surface that represents the cross-section of a part in tension. The maximum normal Stress is 0.174 Mpa and minimum normal Stress is 0.019344 Mpa.

4) Shear Stress

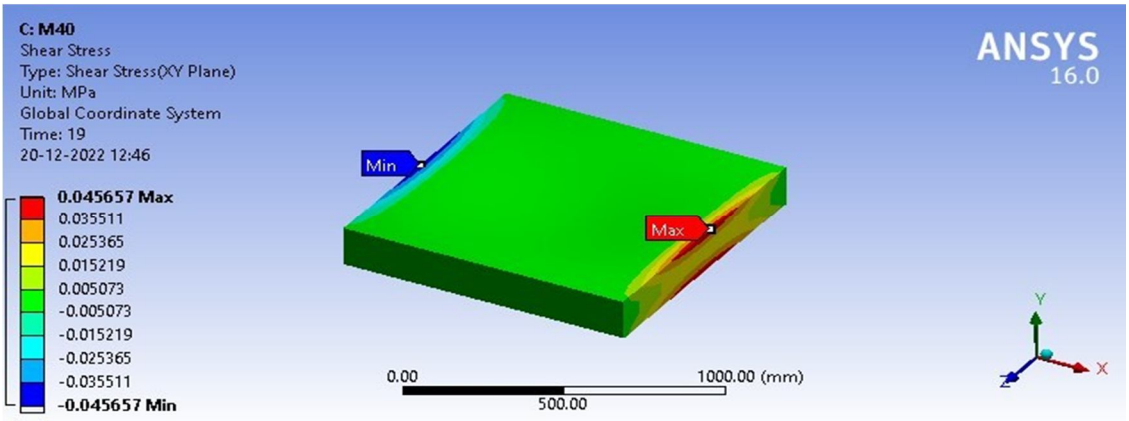


Figure.15 Shear Stress

Shear stress, force tending to cause deformation of a material by slippage along a plane or planes parallel to the imposed stress. The maximum shear Stress is 0.04565 Mpa and minimumshear Stress is 0.005073 Mpa.

5) Maximum Shear Elastic Strain

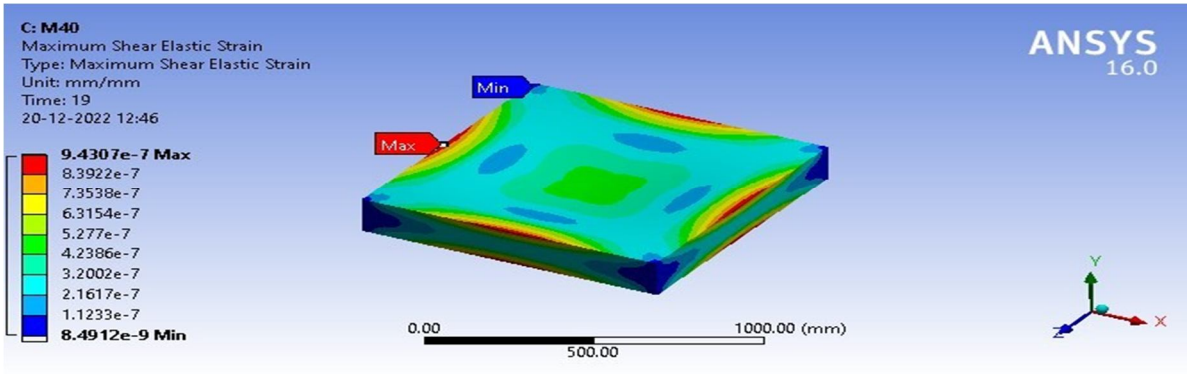


Figure.16 Maximum Shear Elastic Strain

Shear strain is measured as a change in angle between lines that were originally perpendicular.The maximum Shear Elastic Strain is 9.43 x 10^{-7} mm and minimum Shear Elastic Strain is 8.49 x 10^{-9} mm.

D. Analytical Results For M50

1) Total deformation

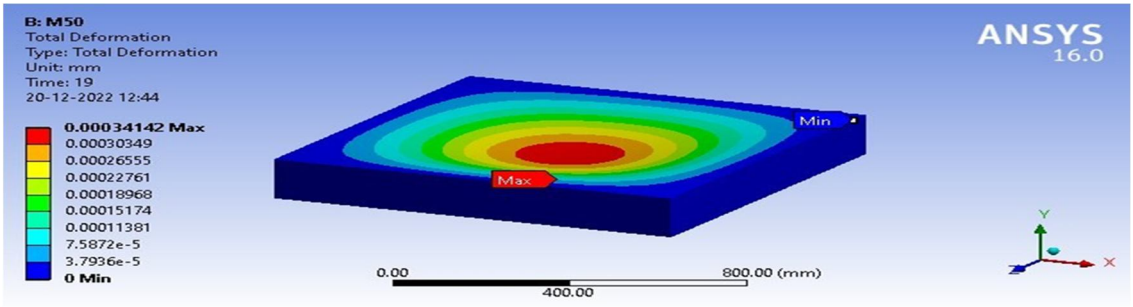


Figure.17 Total deformation

The inclusion of total deflection means that ANSYS accounts for changes in stiffness due to changes in the shape of the parts you are simulating. The maximum deformation is 3.41 x 10^{-4}mm and minimum deformation is 3.79 x 10^{-5}mm.

2) Equivalent Stress

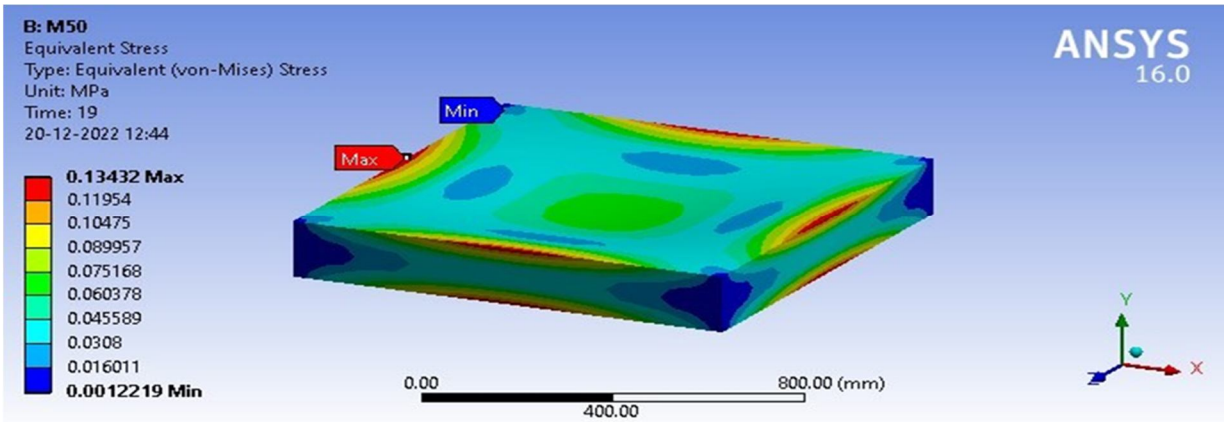


Figure.18 Equivalent Stress

Equivalent stress is widely used to represent a material's status for ductile material. Engineers use this simple scalar value to determine if the material has yield or failed. The maximum Equivalent Stress is 0.13432 Mpa and minimum Equivalent Stress is 0.00122 Mpa.

3) Normal Stress

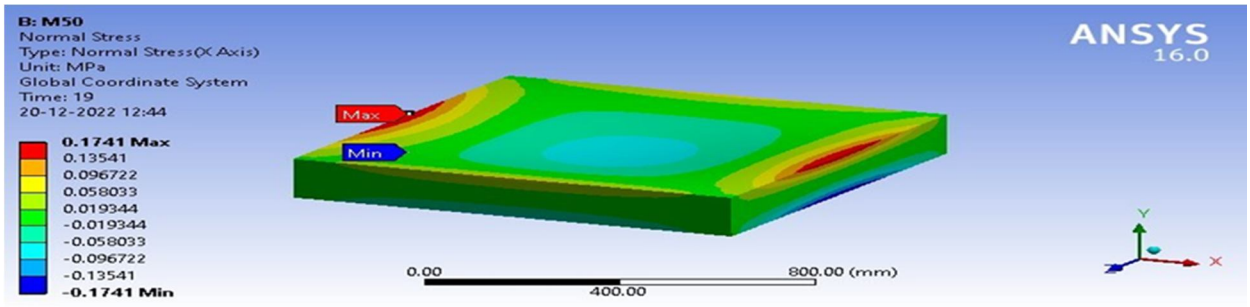


Figure.19 Normal Stress

Normal Stress might be useful is when you request stress on a surface that represents the cross-section of a part in tension. The maximum normal Stress is 0.1741 Mpa and minimum normalStress is 0.0193 Mpa.

4) Shear Stress

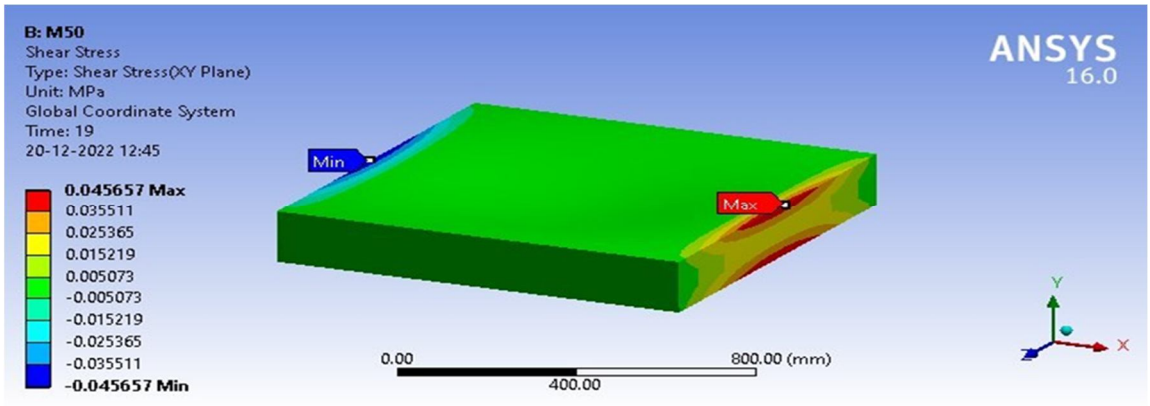


Figure.20 Shear Stress

Shear stress, force tending to cause deformation of a material by slippage along a plane or planes parallel to the imposed stress. The maximum shear Stress is 0.045657 Mpa and minimum shear Stress is 0.0050 Mpa.

5) Maximum Shear Elastic Strain

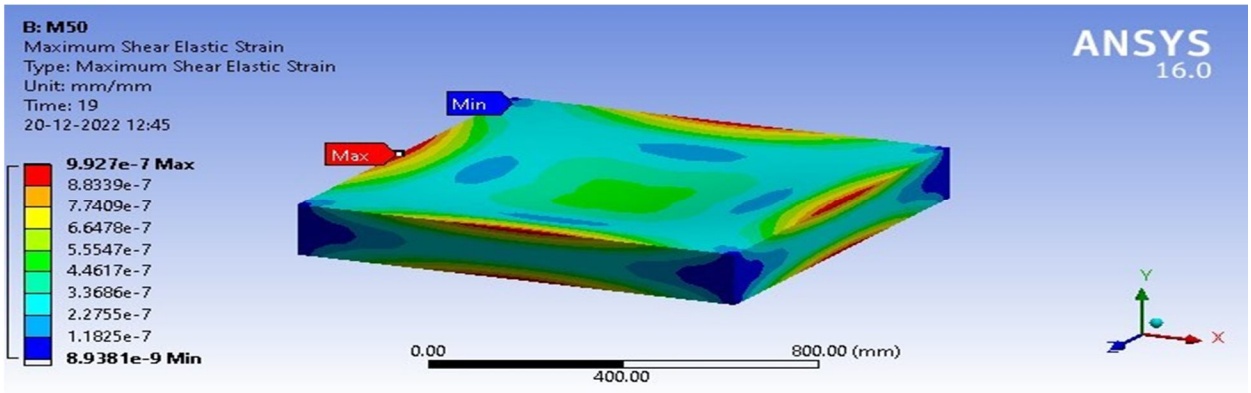


Figure.21 Maximum Shear Elastic Strain

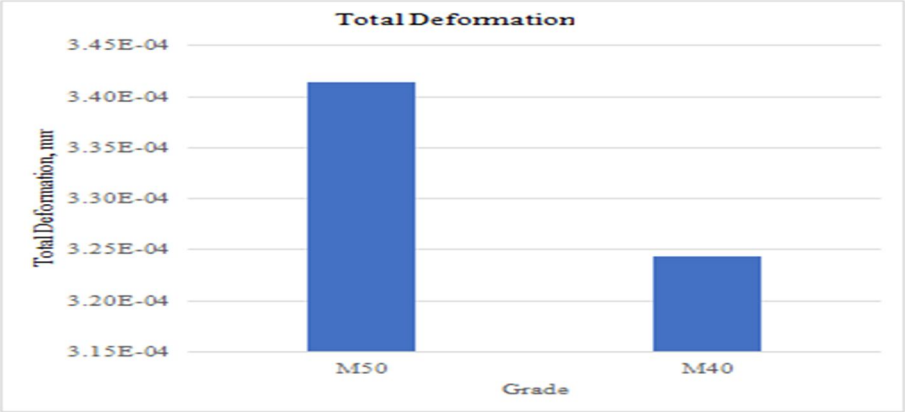
Shear strain is measured as a change in angle between lines that were originally perpendicular.The maximum Shear Elastic Strain is 9.927 x 10^{-7} Mpa and minimum Shear Elastic Strain is 1.1825 x 10^{-7} mm.

E. Graphical Results

1) Total deformation

Table.1 Total Deformation

Total Deformation, mm	
M50	M40
3.41 x 10^{-4}	3.24 x 10^{-4}



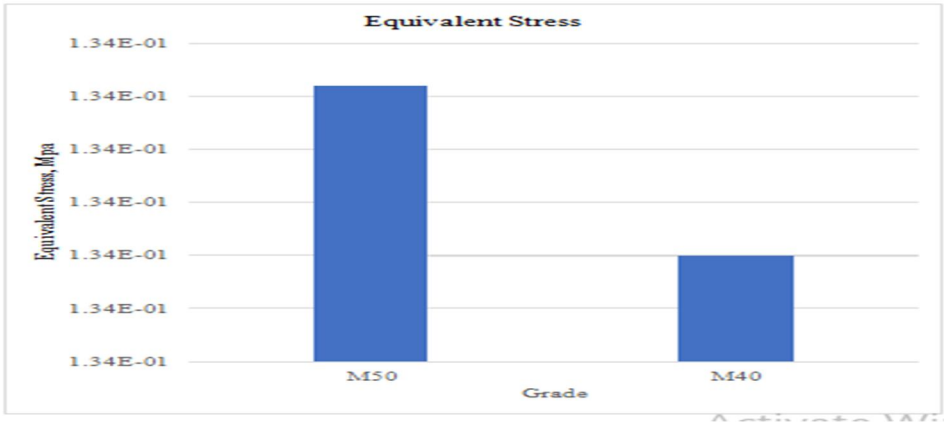
Graph 1. Total Deformation

The graphs show the results for total deformation of M50 & M40 Grades. The maximum deformation in M50 is 3.41x 10^{-4} mm and minimum deformation in M50 is 3.79 x 10^{-4} mm. The maximum deformation in M40 is 3.24 x 10^{-4} mm and minimum deformation in M40 is 3.60 x 10^{-4} mm. As per Comparison maximum deformation is in M50 grade compared to M40grade concrete. So that M40 is suitable for further design.

2) Equivalent Stress

Table.2 Equivalent Stress

Equivalent Stress, Mpa	
M50	M40
1.34 x 10^{-1}	1.34 x10^{-1}



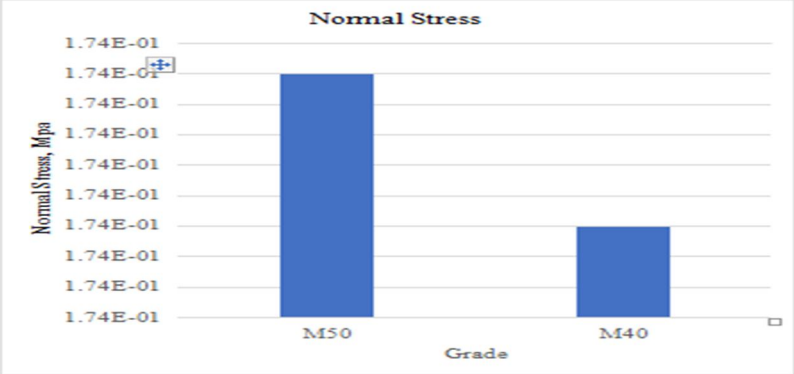
Graph 2. Equivalent Stress

The graphs show the results for Equivalent Stress of M50 & M40 Grades. The maximum Equivalent Stress in M50 is 1.34 x 10^{-1} Mpa and minimum Equivalent Stress in M50 is 0.00122 Mpa. The maximum Equivalent Stress in M40 is 1.34 Mpa and minimum Equivalent Stress inM40 is 0.001219 Mpa. As per Comparison Maximum Equivalent Stress is in M50 grade.

3) Normal Stress

Table.3 Normal Stress

Normal Stress, Mpa	
M50	M40
1.74 x 10^{-1}	1.74 x 10^{-1}



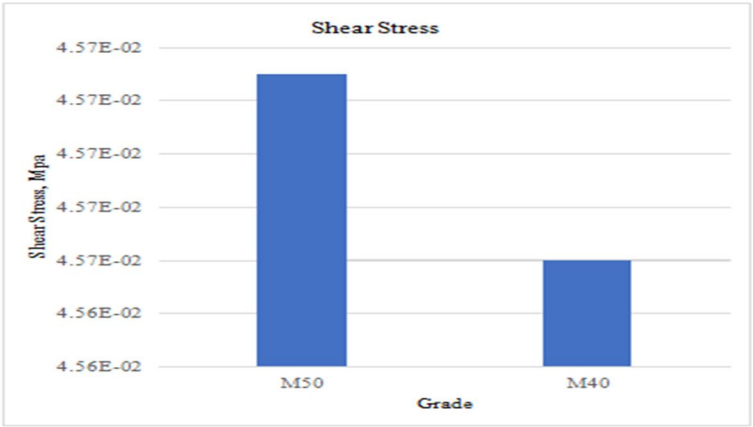
Graph 3. Normal Stress

Normal stresses are the stresses which are perpendicular surface of concrete. Normal Stress ofM50 & M40 Grades are analyzed with help of Ansys workbench and the profile is show in thebar chart format. The maximum normal Stress in M50 is 0.1741 Mpa and minimum normal Stress in M40 is 0.0174 Mpa. As per graphical comparison maximum normal Stress is M40 &M50 grade doesn't show any difference it is possibility that stresses acting on plane are uniformthroughout.

4) Shear Stress

Table.4 Shear Stress

Shear Stress, Mpa	
M50	M40
4 x 10^{-2}	4.57 x10^{-2}



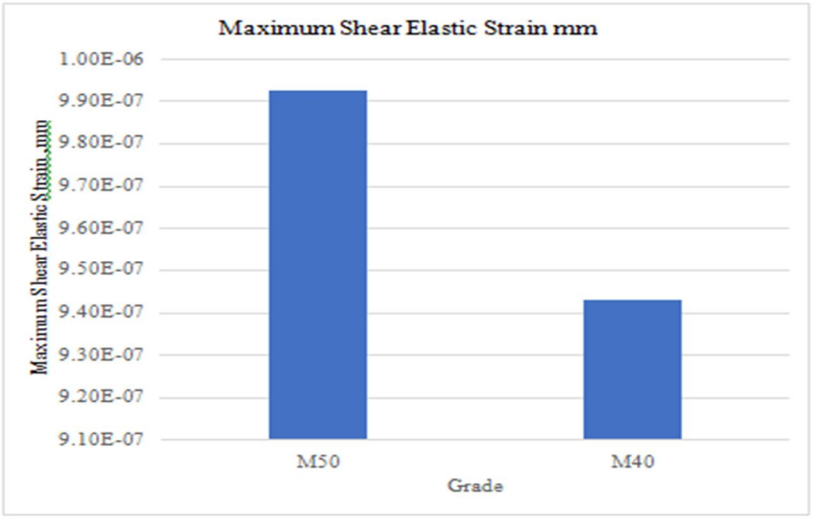
Graph 4. Shear Stress

Shear Stress of M50 & M40 Grades are calculated with the Ansys workbench. The maximum shear Stress in M50 is 4.56 x 10^{-2} Mpa and minimum shear Stress in M50 is 4.56 x 10^{-2} Mpa. The maximum shear Stress in M40 is 4.56 x 10^{-2} Mpa and minimum shear Stress in M40 is 5.07 x 10^{-2} Mpa. As per Comparison Maximum Shear Stress is in M50 grade.

5) Maximum Shear Elastic Strain

Table.5 Maximum Shear Elastic Strain

Maximum Shear Elastic Strain, mm	
M50	M40
9.93 x10^{-7}	9.43 x 10^{-7}



Graph 5. Maximum Shear Elastic Strain

Shear Elastic Strain has relationship of substance that express ratio between force per unit areathat deforms substance. The maximum Shear Elastic Strain in M50 is 9.92 x 10^{-7} Mpa and minimum Shear Elastic Strain in M40 is 9.45 x 10^{-7} mm.

F. Thermal Stress Analysis From Year (2012 To 2021)

M 40

1) Total Deformation (MM)

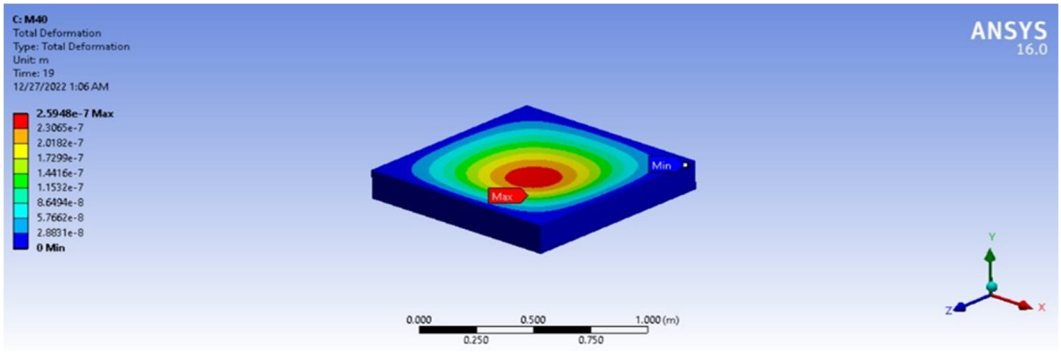


Figure.22 Total Deformation (MM)

The inclusion of total deflection means that ANSYS accounts for changes in stiffness due to changes in the shape of the parts you are simulating. The maximum deformation is 2.59 x 10^{-7}mm and minimum deformation is 2.88 x 10^{-5} mm.

2) Equivalent Stress (MPA)

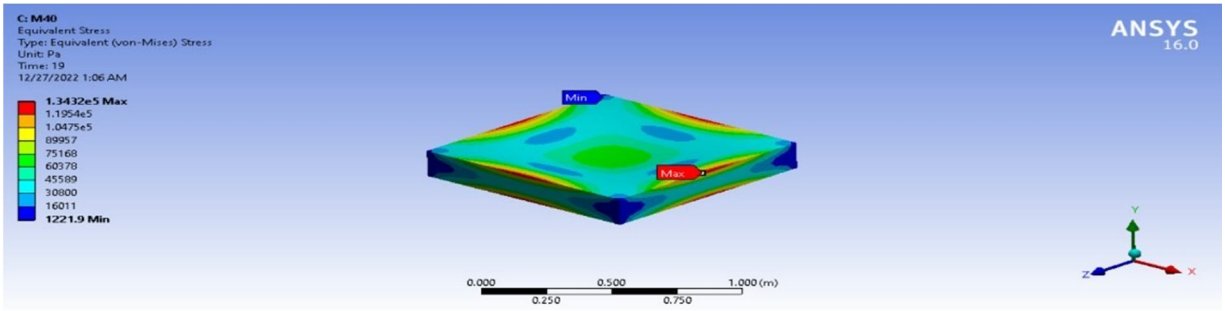


Figure.23 Equivalent Stress (MPA)

Equivalent stress is widely used to represent a material's status for ductile material. Engineers use this simple scalar value to determine if the material has yield or failed. The maximum Equivalent Stress is 0.13432 Mpa and minimum Equivalent Stress is 0.0012219 Mpa.

3) Normal Stress (MPA)

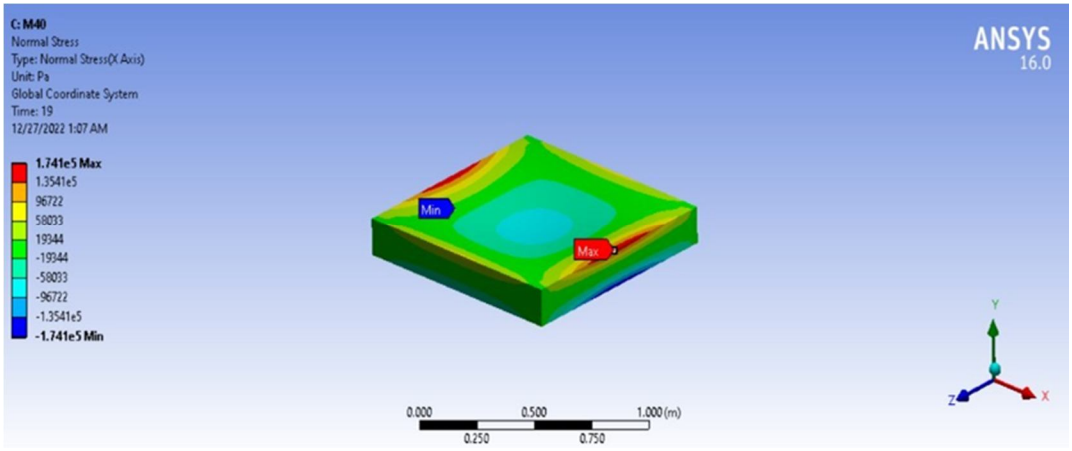


Figure.24 Normal Stress (Mpa)

Normal Stress might be useful is when you request stress on a surface that represents the cross-section of a part in tension. The maximum normal Stress is 0.1741 Mpa and minimum normalStress is 0.1741 Mpa.

4) Shear Stress

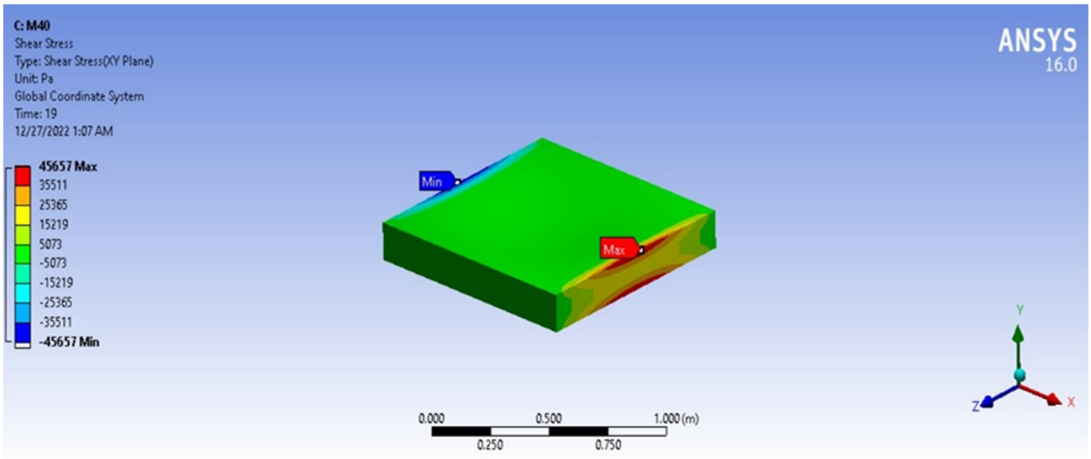


Figure.25 Shear Stress (Mpa)

Shear stress, force tending to cause deformation of a material by slippage along a plane or planes parallel to the imposed stress. The maximum shear Stress is 0.045657 Mpa and minimum shear Stress is -0.045657 Mpa.

5) Maximum Shear Elastic Strain

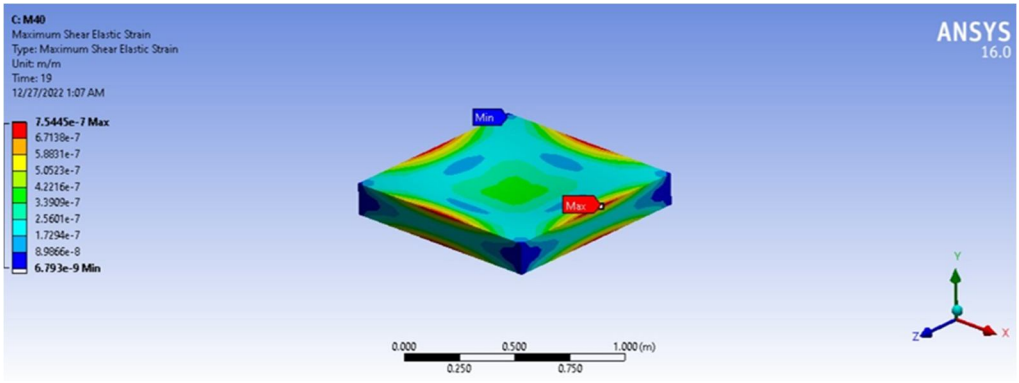


Figure.26 Maximum Shear Elastic Strain (mm)

Maximum Shear Elastic strain is measured as a change in angle between lines that were originally perpendicular. The maximum Shear Elastic Strain is 7.54 x 10^{-7} Mpa and MaximumShear Elastic Strain is 6.79 x 10^{-9} mm. 4.7.2 M50

6) Total Deformation

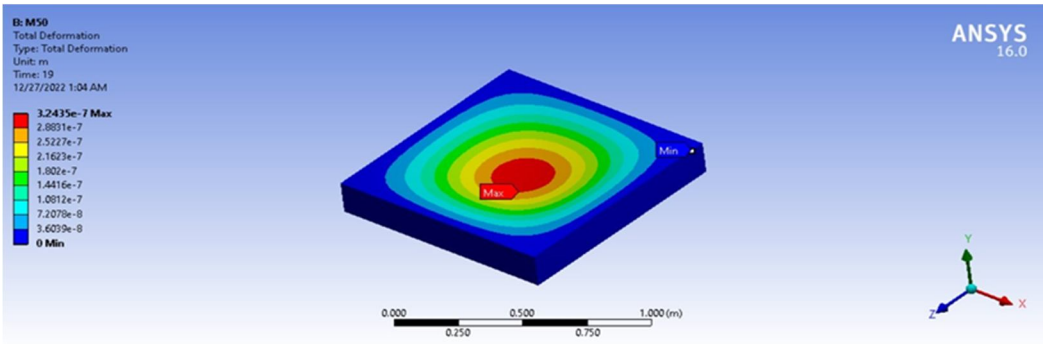


Figure.27 Total Deformation (mm)

The inclusion of total deflection means that ANSYS accounts for changes in stiffness due to changes in the shape of the parts you are simulating. The maximum deformation is 3.24 x10^{-7}mm and minimum deformation is 3.6039 x 10^{-8} mm.

7) Equivalent Stress

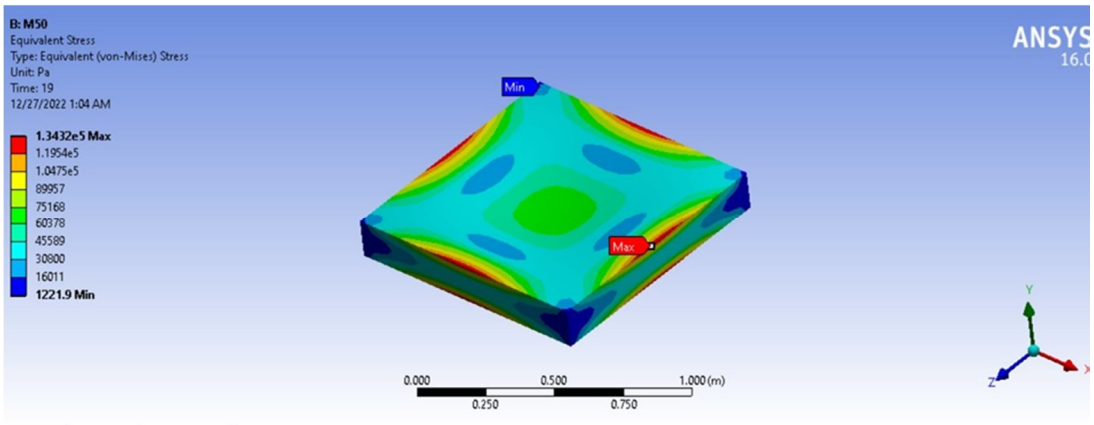


Figure.28 Equivalent Stress (Mpa)

Equivalent stress is widely used to represent a material's status for ductile material. Engineers use this simple scalar value to determine if the material has yield or failed. The maximum Equivalent Stress is 0.13432 Mpa and minimum Equivalent Stress is 0.0012219 Mpa.

8) Normal Stress

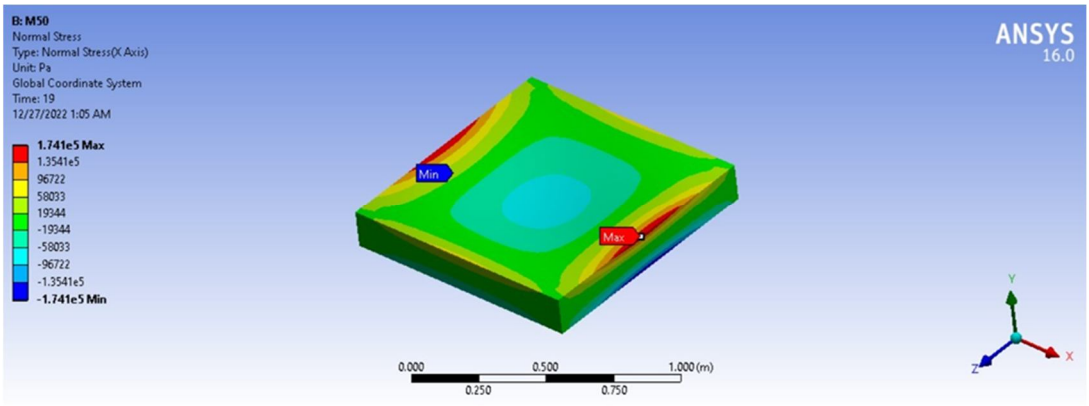


Figure.29 Normal Stress (Mpa)

Normal Stress might be useful is when you request stress on a surface that represents the cross-section of a part in tension. The maximum normal Stress is 0.1741 Mpa and minimum normalStress is -0.1741 Mpa.

9) Shear Stress

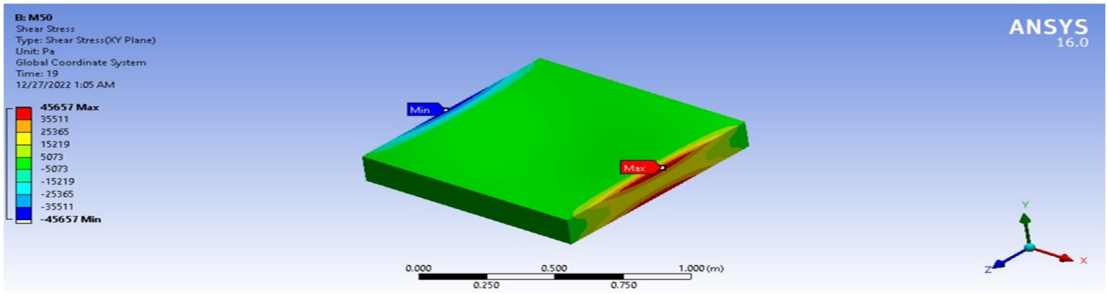


Figure.30 Shear Stress (Mpa)

Shear stress, force tending to cause deformation of a material by slippage along a plane or planes parallel to the imposed stress. The maximum shear Stress is 0.045657 Mpa and minimum shear Stress is -0.045657 Mpa.

10) Maximum Shear Elastic Strain

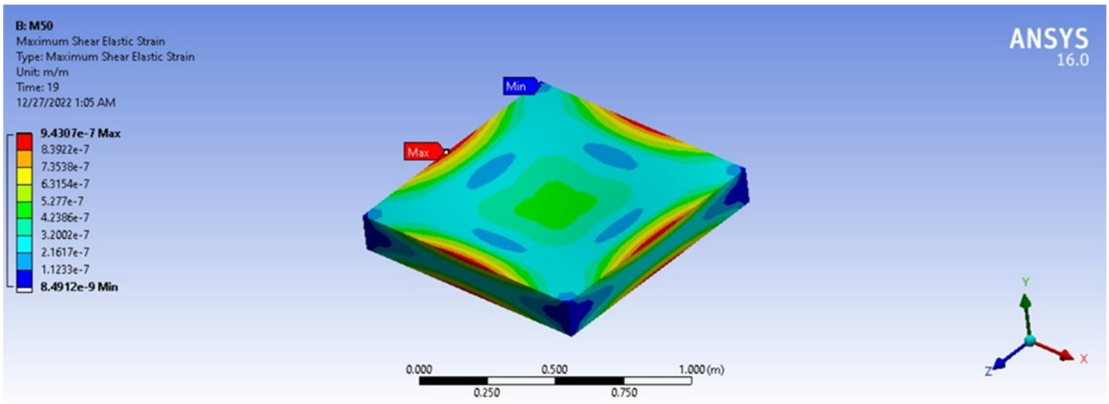


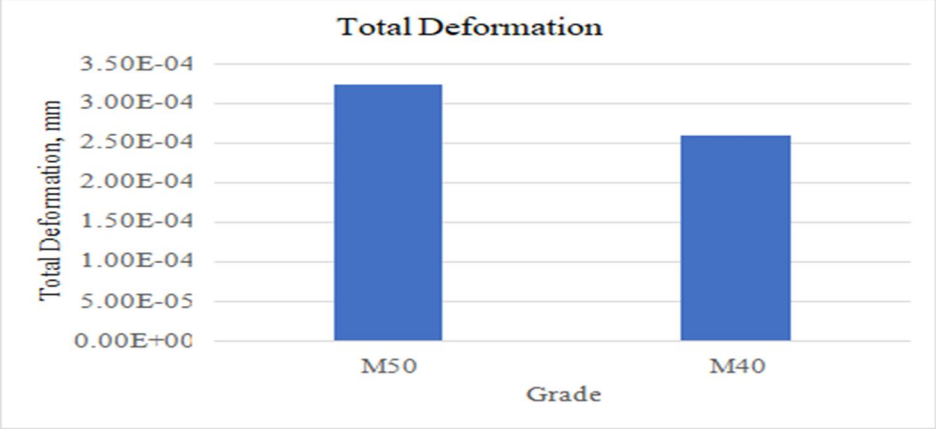
Figure.31 Maximum Shear Elastic Strain (mm)

Maximum Shear Elastic strain is measured as a change in angle between lines that were originally perpendicular. The maximum Shear Elastic Strain is 9.4307 x 10^{-7} Mpa and Maximum Shear Elastic Strain is 8.49 x 10^{-9} mm.

G. Graphical Results

Table.6 Total Deformation (mm)

Time(sec)	Total Deformation, mm	
	M50	M40
1	3.24 x 10^{-4}	2.59 x 10^{-4}

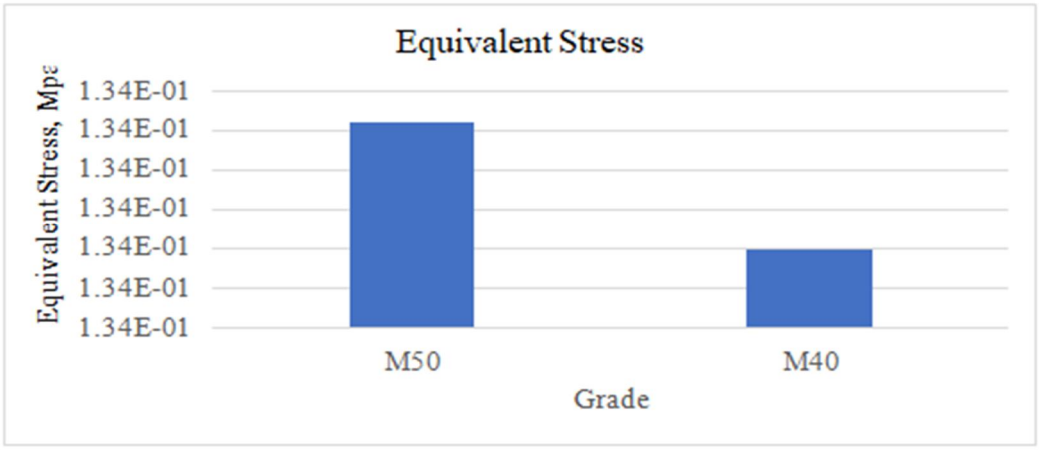


Graph 6. Total Deformation

The Ansys simulation for total deformation of M50 & M40 grades is presented above with graph. The maximum deformation in M50 is 3.31 x 10^{-4} mm and minimum deformation in M50 is 2.88 x 10^{-4} mm. The maximum deformation in M40 is 3.60 x 10^{-4} mm and minimum deformation in M40 is 3.60 x 10^{-4} mm.

Table.7 Equivalent Stress (Mpa)

Time (sec)	Equivalent Stress (Mpa)	
	M50	M40
1	1.34 x 10^{-1}	1.34 x 10^{-1}



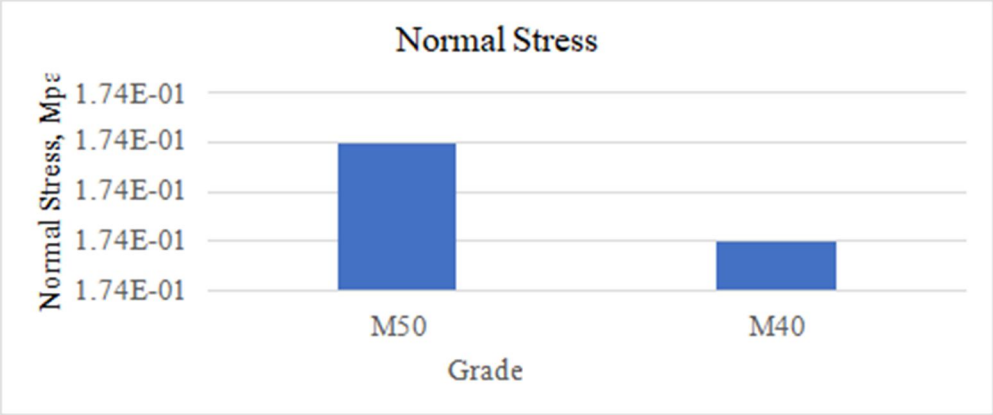
Graph 7. Equivalent Stress

©IJRASET: All Rights are Reserved | SJ Impact Factor 7.538 | ISRA Journal Impact Factor 7.894 |

The graphs show the results for Equivalent Stress of M50 & M40 Grades. The maximum Equivalent Stress in M50 is 1.35 x 10^{-1} Mpa and minimum Equivalent Stress in M50 is 1.74 x 10^{-1} Mpa. The maximum Equivalent Stress in M40 is 1.34 x 10^{-1} Mpa and minimum EquivalentStress in M40 is 0.0012219 Mpa. As per Comparison Maximum Equivalent Stress is in M50 grade.

Table.8 Normal Stress (Mpa)

Time(sec)	Normal Stress (Mpa)	
	M50	M40
1	1.74 x 10^{-1}	1.74 x 10^{-1}

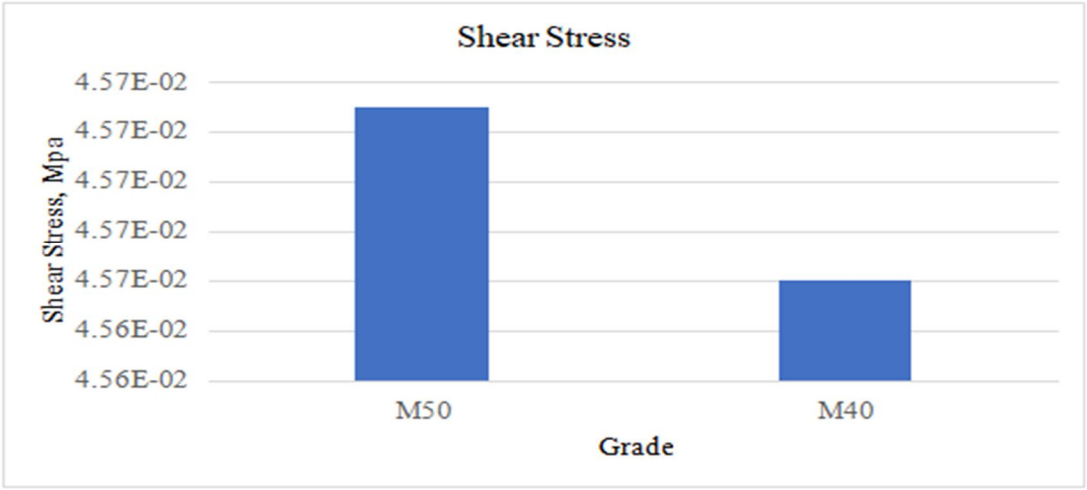


Graph 8. Normal Stress

The graphs show the results for Normal Stress of M50 & M40 Grades. The maximum normalStress in M50 is 0.174 x 10^{-1} Mpa and minimum normal Stress in M50 is 1.74 x 10^{-1} Mpa.

Table.9 Shear Stress (Mpa)

Time(sec)	Shear Stress (Mpa)	
	M50	M40
1	4.57 x 10^{-2}	4.57 x 10^{-2}

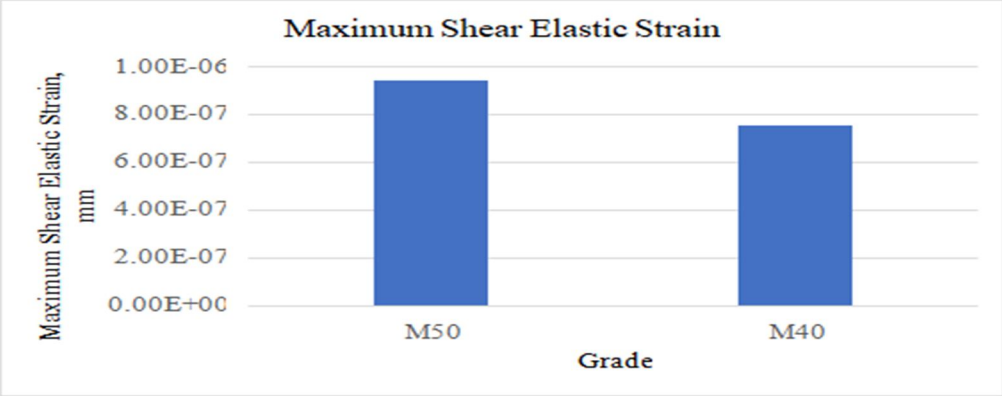


Graph 9. Shear Stress

The graphs show the results for Shear Stress of M50 & M40 Grades. The maximum shearStress in M50 is 4.57 x 10^{-2} Mpa and minimum shear Stress in M50 is 4.57 x 10^{-2} Mpa.

Table 10. Maximum Shear Elastic Strain (mm)

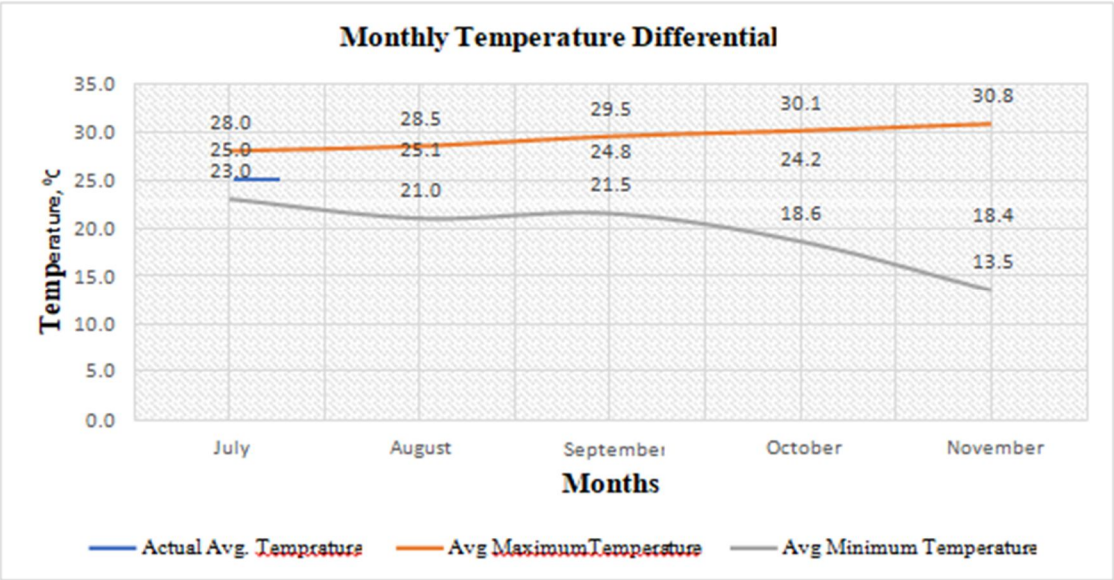
Time(sec)	Maximum Shear Elastic Strain (mm)	
	M50	M40
1	9.43E-07	7.54E-07



Graph 10. Maximum Shear Elastic Strain

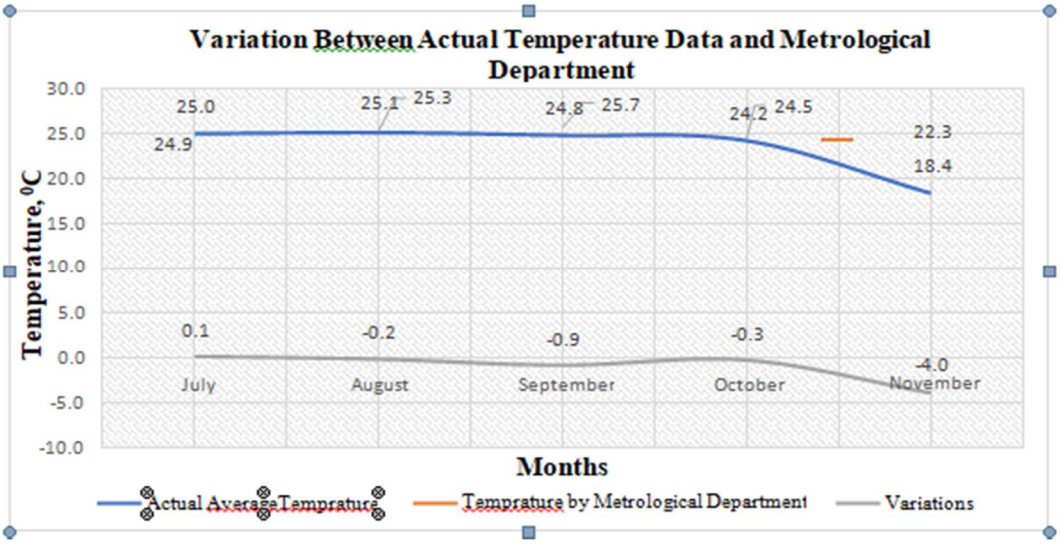
The graphs show the results for maximum Shear Elastic Strain of M50 & M40 Grades. The maximum Shear Elastic Strain in M50 is 9.97 x 10^{-7} Mpa and minimum Shear Elastic Strain inM50 is 6.79 x x10^{-9} mm. The maximum Shear Elastic Strain in M40 is 9.43 x 10^{-7} Mpa and minimum Shear Elastic Strain in M40 is 8.49 x 10^{-9} mm. As per Comparison Maximum ShearElastic Strain is in M50 grade.

H. Temperature Differential Data



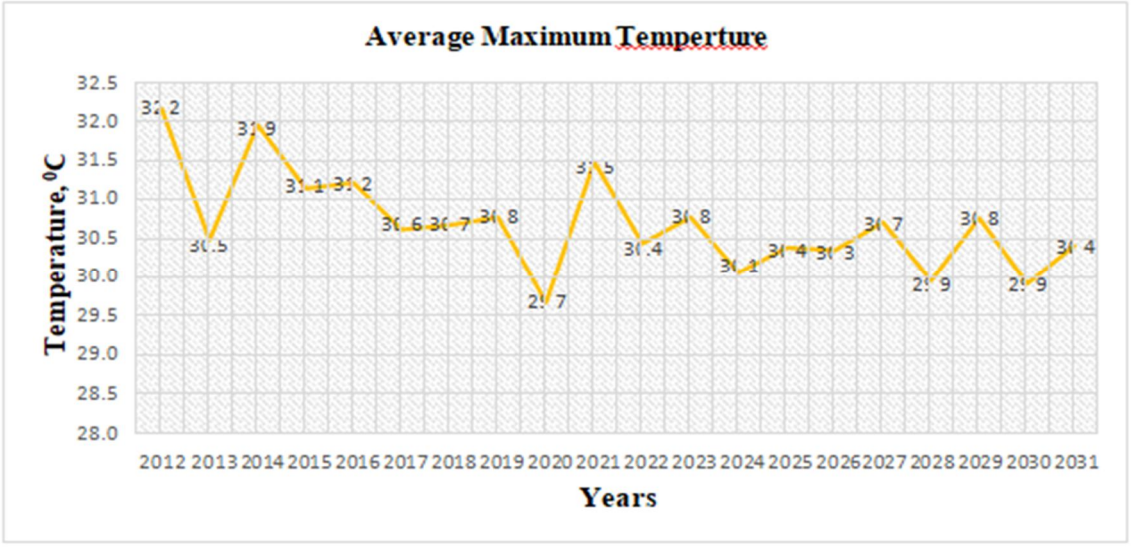
Graph 11. Monthly Temperature Differential

As shown in above Graph, Monthly temperature differential July month Average maximum temperature is 28.0, Average minimum temperature is 23.0 and actual temperature is 25.0. As well as August Month Average maximum temperature is 28.5, Average minimum temperature is 21.0 and actual temperature is 25.1. September Month Average maximum temperature is 29.5, Average minimum temperature is 21.5 and actual temperature is 24.8. October Month Average maximum temperature is 30.1, Average minimum temperature is 18.6 and actual temperature is 24.2. November Month Average maximum temperature is 30.8, Average minimum temperature is 13.5 and actual temperature is 18.4.



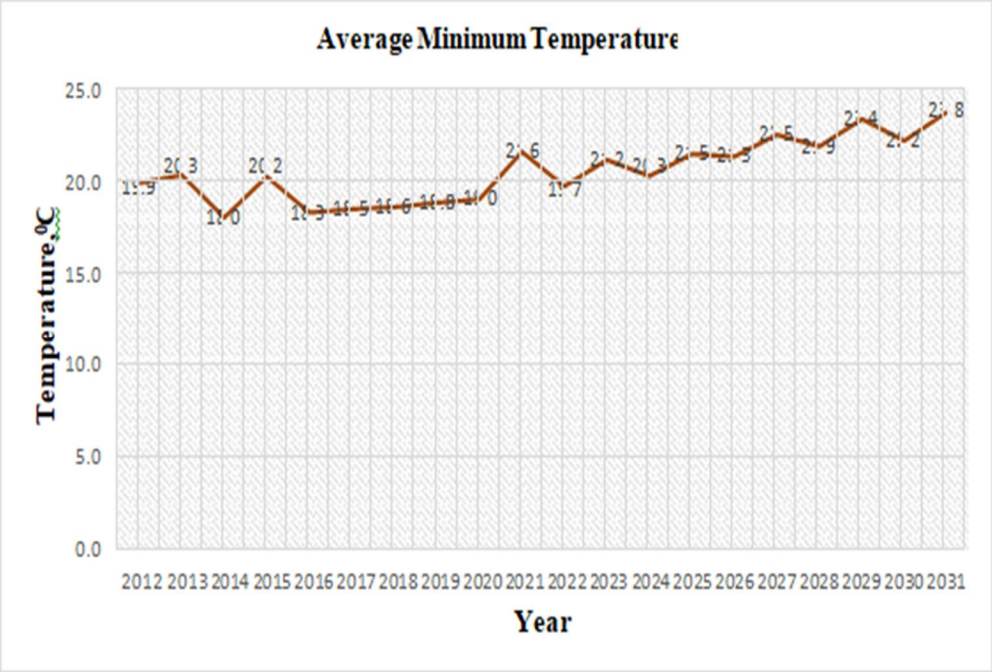
Graph 12. Variation between Actual Temperature Data and Metrological Department

As shown in above graph, calculate the temperature between actual Data and metrological department temperature Data. In July month actual average temperature 25.0, temperature by metrological department is 24.9 and Difference between actual temperature and metrological department temperature is 0.1. As well as August month actual average temperature 25.1, temperature by metrological department is 25.3 and Difference between actual temperature and metrological department temperature is -0.2. September month actual average temperature 24.8, temperature by metrological department is 25.7 and Difference between actual temperature and metrological department temperature is -0.9. October month actual average temperature 24.2, temperature by metrological department is 24.5 and Difference between actual temperature and metrological department temperature is -0.3. November month actual average temperature 18.4, temperature by metrological department is 22.3 and Difference between actual temperature and metrological department temperature is -4.0.



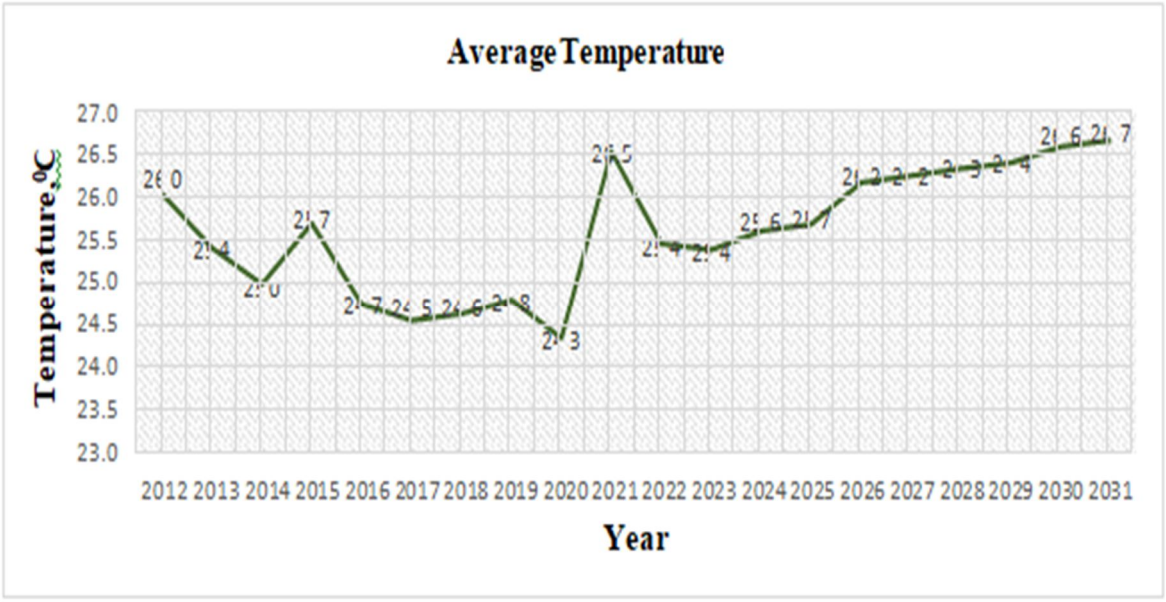
Graph 13. Average Maximum Temperature

As shown in above graph. Calculate year 2012 to year 2031 Average Maximum temperature. Year 2012 Average Maximum Temperature 32.2. as well as Year 2022 Average Maximum temperature is 30.4 and year 2031 Average Maximum temperature is 30.4.



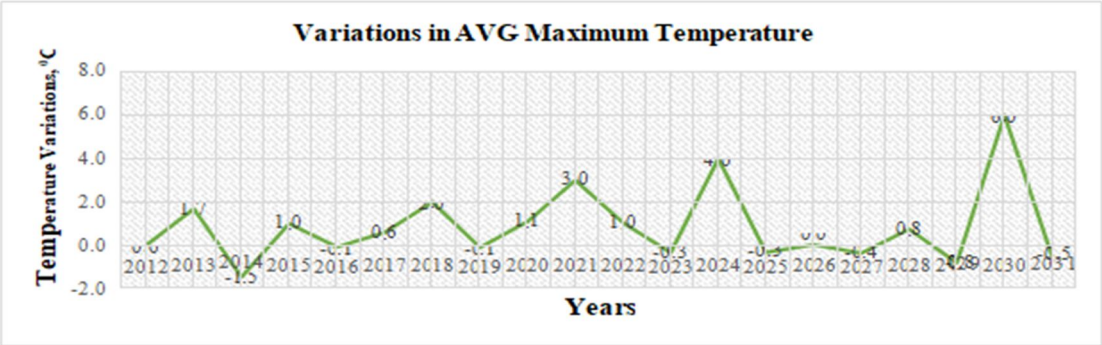
Graph 14. Average Minimum Temperature

As shown in above graph. Calculate year 2012 to year 2031 Average Minimum Temperature. Year 2012 Average Maximum Temperature 19.9. As well as Year 2022 Average Minimum temperature is 19.7 and year 2031 Average Minimum temperature is 23.8.



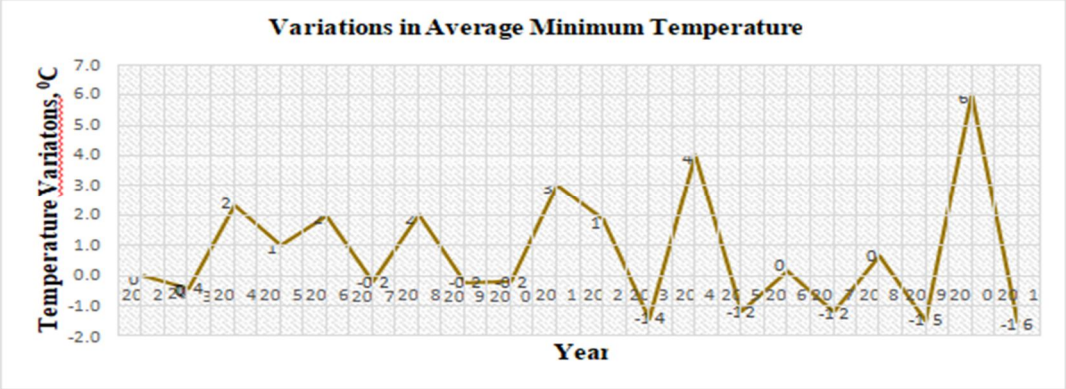
Graph 15. Average Temperature

As shown in above graph. Calculate year 2012 to year 2031 Average Temperature. Year 2012Average Temperature 26.0. as well as Year 2022 Average Temperature is 25.4 and year 2031Average Temperature is 26.7.



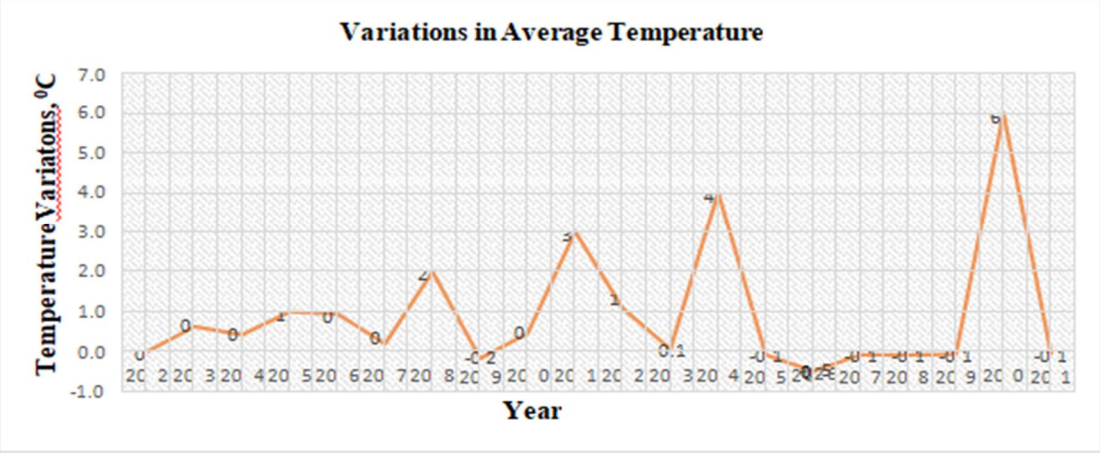
Graph 16. Variations in Average Maximum Temperature

As shown in above graph. Calculate year 2012 to year 2031 Variation in Average Maximum Temperature. Year 2012 Average Maximum Temperature 0.0. as well as Year 2022 Variation in Average Maximum temperature is 1.0 and year 2031 Variation in Average Maximum temperature is 0.5.



Graph17. Variations in Average Minimum Temperature

As shown in above graph. Calculate year 2012 to year 2031 Variation in Average Minimum Temperature. Year 2012 Average Minimum Temperature 0.0. as well as Year 2022 Variationin Average Minimum Temperature is 1.9 and year 2031 Variation in Average Minimum Temperature is 1.6.



Graph 18. Variations in Average Temperature

As shown in above graph. Calculate year 2012 to year 2031 Variation in Average Temperature.Year 2012 Average Temperature 0.0. as well as Year 2022 Variation in Average Temperatureis 1.1 and year 2031 Variation in Average Temperature is -0.1.

©IJRASET: All Rights are Reserved | SJ Impact Factor 7.538 | ISRA Journal Impact Factor 7.894 |

V. CONCLUSION

1) This study is done to perform analysis on temperature differential for rigid pavement (mainly for PQC layer). In IRC: 58-2015 table 1 provides temperature differential for several regions in India. It provides temperature differential values to design pavement slabs of various thicknesses. But at the bottom of table, it also mentions that data provided is by Central Road Research Institute New Delhi in 1974. Which is almost 50 years old, this analysis is carried out for comparison between temperature differential of that table & current temperature. This analysis is performed in Pune region which falls under Maharashtra state. To carry out this analysis Digital Temperature Sensors are used. Specimens of concrete grade M40 are constructed and sensors are installed into them at near the top and & bottom position to monitor temperature. Temperature from July to November is collected and compared with metrological department data.

2) It is observed that temperature readings collected by temperature sensor are nearly similar to data shown by metrological department. (Temperature Data from July to November). After Confirming data is collected is same as IMD, further analysis is done by collecting previous 10 years' data (2012 to 2021). Based on that data future 10 years' temperature differential is predicted (2022 to 2031). Data has shown increase in minimum as well as maximum temperature differential when compared to IRC.

3) Surface expansion cracks form as a result of the adverse effects of temperature change on inflexible pavement. It is necessary to evaluate the changes in pavement performance under temperature variation and hypothesized temperature impacts. Temperature measurements are used in the evaluation and design of pavements. Analytical Results for M40 model and Analytical Results for M50 model were computed in the study. As a result, the M50 model suffered the most fatigue damage, while the M40 model suffered the least. As a consequence, a comparison was made between the M40 model and the M50 model. In contrast, the M40 model is more effective than the M50 model.

4) Pavement design is also prepared to test the temperature differential readings for Maharashtra state by assuming design and traffic conditions. Also, trial thickness is Effect of Temperature Variation on Rigid Pavement by Using Sensor assumed and later modified to create safe pavement design. Average temperature is 25.1 0C which is average of years from 2018 to 2022. From design proposed thickness for that temperature is 350mm, which is safe.

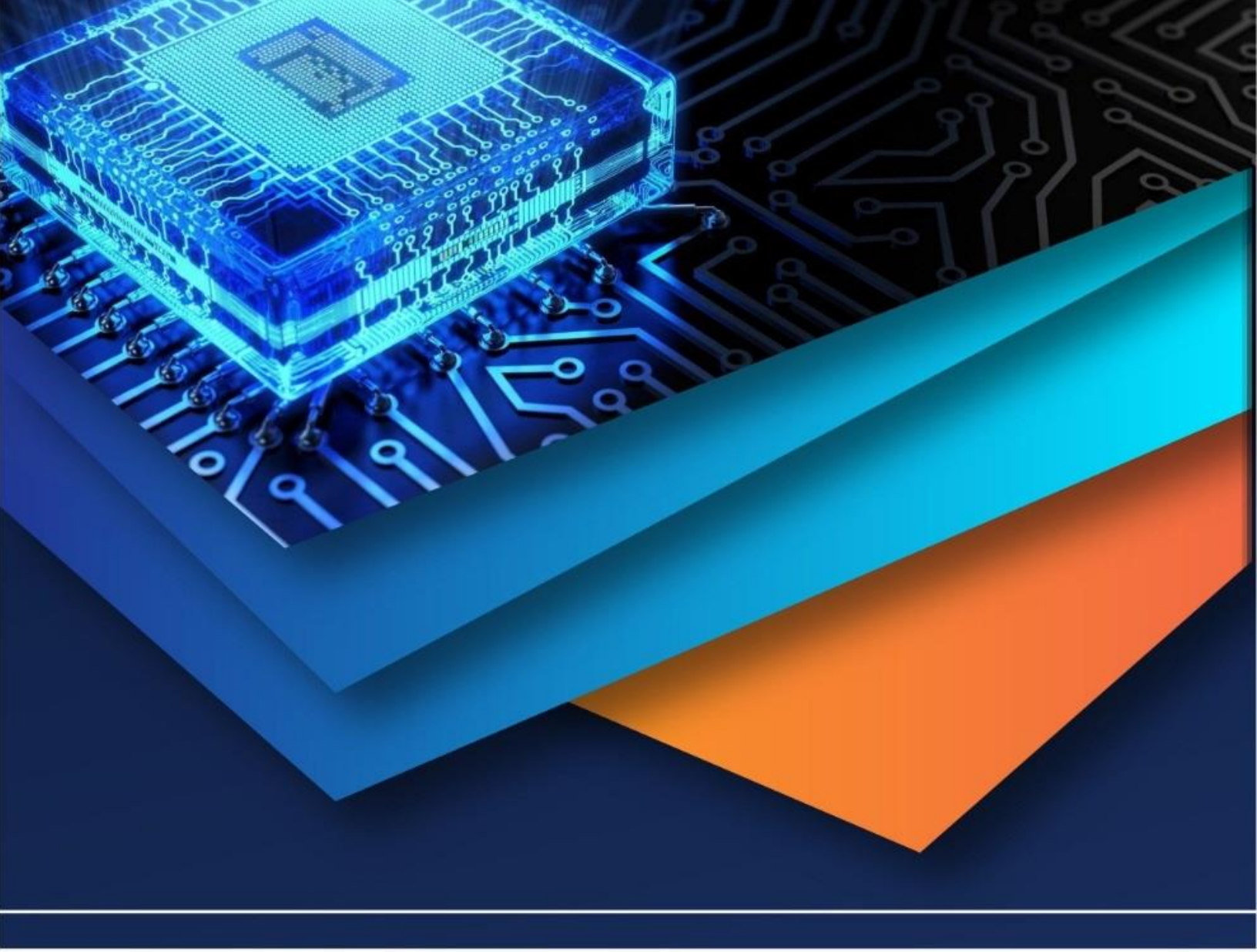
5) This study encourages pavement designers to reconsider temperature differentials while doing warping stress calculations.

REFERENCES

[1] Bianchini, A. (2013). Evaluation of temperature-induced curling in concrete slabs using deflection difference analysis. Journal of Transportation Engineering, 139(2), 130–137.
[2] Gupta S., Lin Y. A., Lee, H. J., Buscheck, J., Wu, R., Lynch, J. P., Garg, N., & Loh, K.
[3] J. (2021). In situ crack mapping of large-scale self-sensing concrete pavements using electrical resistance tomography. Cement and Concrete Composites, 122, 104154.
[4] Giuseppina Uva, Francesco Porco, Andrea Fiore, Giacinto Porco (2014). Structural monitoring using fiber optic sensors of a pre-stressed concrete viaduct during construction phases. Case Studies in Nondestructive Testing and Evaluation, 2(1), 27–37.
[5] Hiller, J. E., & Roesler, J. R. (2010). Simplified nonlinear temperature curling analysis for jointed concrete pavements. Journal of Transportation Engineering, 136(7), 654– 663.
[6] Hu, J., Wang, K., & Bektas, F. (2014). Monitoring of Joint Cracking Development in Concrete Pavement with Concrete Embedment Strain Gages. 147–154.
[7] Huang, K., Zollinger, D. G., Shi, X., & Sun, P. (2017). A developed method of analyzing temperature and moisture profiles in rigid pavement slabs. Construction and Building Materials, 151, 782–788.
[8] Li Y., Liu L., & Sun L. (2018). Temperature predictions for asphalt pavement with thick asphalt layer. Construction and Building Materials, 160, 802–809.
[9] Loganathan K., & Souliman M. I. (2017). Prediction of average annual surface temperature for both flexible and rigid pavements. 4, 259–267.
[10] Mohod M. Kadam K. (2016). A Review on Critical Stresses in Concrete Pavement. National Conference on Advance in Construction Technology and Management 19- 20th February, 2016 VNIT Nagpur, February.
[11] Masud M. M., & Haider S. W. (2020). Impact of Moisture Infiltration on Rigid Pavement Performance and Optimum Timing for resealing of Damaged Joints IRF GLOBAL R2T Conference. November.
[12] P. J., Balasubramanian, R., Miller, H., Viall, B., Igoe, P., & Eftekhari, S. (2017). Wireless Subsurface Sensors Supporting Remote Roadway Management. 491–498.
[13] Pandey V. K. Student, M. T., Engineering, C., & Engineering, F. (2021). A Review on Failure of Rigid Pavement. 01, 548–553.
[14] Pour-Ghaz M., Barrett T., Ley T., Materer N., Apblett A., & Weiss J. (2014). Wireless Crack Detection in Concrete Elements Using Conductive Surface Sensors and Radio Frequency Identification Technology. Journal of Materials in Civil Engineering, 26(5),923–929.
[15] Schwartz C. W., Cetin B., Forman B. A., & Ruppelt B. (2018). Performance of Different Climate Data Sources in Mechanistic-Empirical Pavement Distress Analyses. Journal of Transportation Engineering, Part B: Pavements, 144(1), 04017023.
[16] Shtayat A., Moridpour S., Best B., Shroff A., & Raol D. (2020). A review of monitoring systems of pavement condition in paved and unpaved roads. Journal of Traffic and Transportation Engineering (English Edition), 7(5), 629–638.

[17] Somani P., & Gaur A. (2020). Evaluation and reduction of temperature stresses in concrete pavement by using phase changing material. Materials Today: Proceedings, 32, 856–864.
[18] Vaitkus A., Žalimiene L., Židanavičiute J., & Žilioniene D. (2019). Influence of temperature and moisture content on pavement bearing capacity with improved subgrade. Materials, 12(23).
[19] Yeon J. H., Choi S., Ha S. & Won M. C. (2013). Effects of creep and built-in curling on stress development of Portland cement concrete pavement under environmental loadings. Journal of Transportation Engineering, 139(2), 147–155.
[20] Zhao H., Wu Z., Wang S., Zheng J., & Che G. (2011). Concrete pavement deicing withcarbon fiber heating wires. Cold Regions Science and Technology, 65(3), 413–420.

©IJRASET: All Rights are Reserved | SJ Impact Factor 7.538 | ISRA Journal Impact Factor 7.894 |



10.22214/IJRASET

45.98

IMPACT FACTOR: 7.129

IMPACT FACTOR: 7.429

INTERNATIONAL JOURNAL FOR RESEARCH

IN APPLIED SCIENCE & ENGINEERING TECHNOLOGY

Call : 08813907089 (24*7 Support on Whatsapp)